

# Magnetic horizons of UHECR sources and the GZK feature

Olivier Deligny<sup>a</sup>, Antoine Letessier-Selvon<sup>a</sup>, Etienne Parizot<sup>b</sup>

<sup>a</sup> *LPNHE, Universités de Paris 6 et 7, C.N.R.S., 4 place Jussieu T33 RdC,  
F-75252 Paris Cedex 05, France*

<sup>b</sup> *IPN Orsay, Université de Paris 11, C.N.R.S., Orsay Cedex, France*

---

## Abstract

We study the effect of random extra-galactic magnetic fields on the propagation of protons of energy larger than  $10^{19}$  eV. We show that for reasonable field values (in the 100 nG range) the transition between diffusive and ballistic regimes occurs in the same energy range as the GZK cutoff (a few  $10^{19}$  eV). The usual interpretation of the flux reduction above the GZK energy in terms of a sudden reduction of the visible horizon is modified. Moreover, since the size of the diffusion sphere of a continuous source of cosmic rays is of the order of 10 Mpc, the local structure of the Universe and therefore of potential local astrophysical sources plays a dominant role in the expected spectrum. Under reasonable assumptions on the sources configurations the expected GZK cutoff is reduced.

---

## 1 Introduction

The cosmic microwave background is expected to limit the travel distance of nucleons and nuclei above 30 EeV, due to photo-disintegration or photo-production of pions. These interactions impose a cut-off in the spectrum of high-energy cosmic rays known as the GZK cutoff [1], strongly limiting their visible flux.

The usual interpretation of the expected reduction of the flux above 100 EeV lies in the sudden reduction of the visible Universe from a few Gpc below 10 EeV to less than 20 Mpc above a few 100 EeV. This simple view may however be strongly modified in the presence of extra-galactic magnetic fields of the order of 100 nG. Such strong fields are compatible with current observations and upper limits from Faraday rotation measurements which indicate field strengths at the  $\mu\text{G}$  level within the central Mpc region of galaxy clusters [2,3,4,5]. Relatively strong magnetic fields may exist in intergalactic space with coherence lengths of the order of a Mpc.

In realistic models of the Universe, however, such strong fields cannot fill the entire intergalactic volume, and should rather be concentrated along the high density sheets where matter also concentrates, as suggested by large-scale structure formation models [18]. The transport of UHECRs in this kind of environments, and their resulting spectrum observed on Earth, depend on the particular geometry of the fields, combined with that of the sources, and on the intensity of the magnetic fields. This has been investigated by a number of authors using various assumptions for the distance of one or a few local sources, and working out UHECR propagation in a model of the local supercluster [6,7,8,9,10,11]. It has been found that under some circumstances, the UHECR spectrum could show an attenuated GZK suppression.

In this paper, we focus on the effect of strong magnetic fields around our Galaxy, assuming that the local group lies within a supercluster with higher than average magnetic field. In order to obtain a clear physical understanding of this effect alone, we use a spherically symmetric configuration and a homogeneous field in the Universe. This is clearly not representative of the observed walls-and-voids structure of our Universe on all scales, but it allows us to emphasize a basic mechanism using a complete Monte-Carlo propagation model, and disentangling the configuration specific effects from the influence of strong fields.

As a matter of fact, in magnetic fields of a 100 nG, a charged particle of 10 EeV has a Larmor radius of 100 kpc and propagates diffusively while at higher energies (above 100 EeV, say) the trajectories are essentially ballistic. Therefore the clear picture of the GZK cutoff imposed by particle dynamics gets blurred by another effect taking place at the same energy: the transition between ballistic and diffusive transport regimes.

Another point to note is that in such a field and for attenuation times of the order of a few Gyr (attenuation of pre-GZK protons by pair production), the radius of the diffusion sphere of a continuous source is only 10 Mpc. Therefore, far away sources ( $D \geq 100$  Mpc, say), would not be visible at any energy.

Given the above ingredients, nearby sources ( $10 \text{ Mpc} \leq D \leq 100 \text{ Mpc}$ ) appear to be responsible for the observed UHECR spectrum at *all* energies. These sources would be sufficiently far away so that we lie outside their low-energy (1–10 EeV) diffusion spheres, therefore reducing the corresponding flux, but close enough so that their high-energy component does not get significantly attenuated by energy losses. This can reduce the usually inferred flux difference between energies below and above the GZK energy. In addition, on a 10 Mpc scale the Universe cannot be taken as isotropic and uniform, which indicates that the local distribution of matter will play a dominant role in the actually observed energy spectra.

In the following we explore this scenario. The next section describes our magnetic field model and our particle propagation Monte-Carlo. Section 3 discusses the magnetic horizon for charged particles and section 4 presents our results.

## 2 A simplistic magnetized Universe

### 2.1 Field modelling

We simulated a magnetized Universe following the method of [12,13]. Our turbulent field has a zero mean value and fluctuates following a Gaussian distribution. The spectrum of fluctuations is a power law

$$\langle \delta B(\vec{k})^2 \rangle = S_0 k^{-2-\beta}$$

The normalization  $S_0$  is obtained through the Wiener-Kintchine theorem by imposing the average fluctuation strength  $\langle \delta B^2 \rangle$ :

$$\langle \delta B^2 \rangle = \int S_0 k^{-2-\beta} 4\pi k^2 dk$$

leading to

$$S_0 = \frac{\beta - 1}{k_m^{1-\beta} - k_M^{1-\beta}} \langle \delta B^2 \rangle$$

The maximum ( $k_M$ ) and minimum ( $k_m$ ) modes are set respectively by the size of the simulation box  $L_c = 1$  Mpc (related to the coherence length of our field model) and the step size of the grid  $l = 15$  kpc. We used a Kolmogorov fluctuation spectrum corresponding to  $\beta = 5/3$ . In Fourier space, the field verifies  $\vec{B}_k \cdot \vec{k} = 0$  to satisfy  $\text{div} \vec{B} = 0$  and we pick up a random phase in the transverse plane to complete the field description. In real space the field is computed on a 15 kpc grid over a volume of 1 Mpc<sup>3</sup>. This volume is then translated periodically to fill our modelled Universe. The value of the field at any point in space is obtained through a linear interpolation of the 8 closest vertices of the grid.

### 2.2 Particle trajectories and sources spectra

For each Monte-Carlo simulation, we compute a field configuration according to the above method and we follow a number of protons as long as their en-

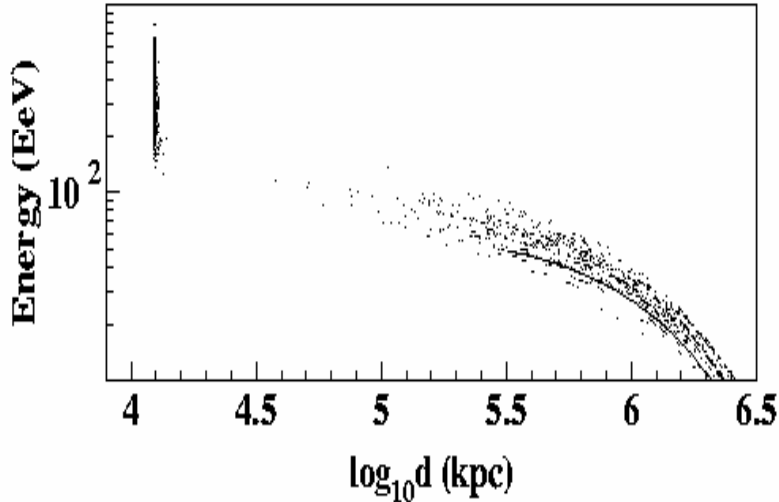


Fig. 1. Particle energies as a function of the distance of travel in a 100 nG field for an observer lying on a sphere 12 Mpc away from the particle source. The initial energy is 800 EeV. On the left, an accumulation of points represents the particles that did not interact and follow a ballistic trajectory; on the right, the solid line represents the expected contribution of the continuous pair-production energy losses.

ergy is above 10 EeV or their propagation time is below 3 Gyr. At each step along their trajectory, we solve the equation of motion in the local field and compute the energy loss due to pion photo-production, simulating each interaction. The losses due to pair production are treated continuously. Neutrons, if produced, are also followed until they transform again into a proton via the photo-production of pions or until they decay.

To compute the spectrum of a source at a given distance  $R$  from the observer, we generate a set of protons at the origin and record the times (and the corresponding energies) of each crossing of a sphere of radius  $R$ , centered on the origin. By construction, our spectrum does not depend on the crossing position on the sphere, therefore we record them all. Moreover the effective detection probability being very small (the surface of a detector is negligible compared to the surface of the sphere), we compute the spectrum at various radii following the same set of particles.

Fig. 1 shows the distribution of particle energies as a function of trajectory length (equivalent to time) for an observer located on a sphere 12 Mpc away from the source, and for an initial energy of 800 EeV.

For radii comparable to or smaller than  $L_c$  the orientation of the field on the surface of the sphere may not average properly and may lead to strong distortion in the time distribution of the particle crossings (a particle trapped along a field line parallel to the sphere surface may cross it many times over a small distance). To avoid this effect we regenerate a field configuration every

100 generated protons.

From the recorded information we are able to compute the probability  $\mathcal{F}(t - t_0, E; R, E_0)dE dt$  for a particle produced at time  $t_0$  with energy  $E_0$  to be detected at a given distance  $R$  at time  $t$  with an energy  $E$ . From these probability tables, and assuming an isotropic distribution of sources  $\rho(R) = \rho_0$ , the spectrum observed today (time  $t$ ) from sources located between  $R_{min}$  and  $R_{max}$  is given by:

$$\frac{dN}{dE}(t) = \rho_0 \int_{R_{min}}^{R_{max}} dV \int_0^t dt_0 \int_{E_0^{min}}^{E_0^{max}} dE_0 f(E_0) \frac{1}{4\pi R^2} \mathcal{F}(t - t_0, E; R, E_0), \quad (1)$$

where  $f(E_0)$  is the source injection spectrum and where we have neglected all cosmological effects.

### 3 Magnetic horizon

As we mentioned in the introduction, for field strengths of the order of 100 nG with Mpc coherence length, particle trajectories below a few tens of EeV are well described by the diffusion equation. Several diffusive regime may be distinguished within a given field configuration, depending on the particle energy. For the pure random field we are considering, three regimes have been identified and can be parameterized with the following diffusion coefficients (in  $\text{Mpc}^2/\text{Myr}$ ) [13]:

$$\begin{aligned} D(E) &\simeq 2 \cdot 10^{-2} \left( \frac{E}{B} \frac{\mu\text{G}}{10^{20}\text{eV}} \right)^{7/3} \left( \frac{L}{\text{Mpc}} \right)^{-4/3} (E > E^*) \\ &\simeq 3 \cdot 10^{-2} \left( \frac{E}{B} \frac{\mu\text{G}}{10^{20}\text{eV}} \right) (0.1E^* < E < E^*) \\ &\simeq 4 \cdot 10^{-3} \left( \frac{E}{B} \frac{\mu\text{G}}{10^{20}\text{eV}} \right)^{1/3} \left( \frac{L}{\text{Mpc}} \right)^{-2/3} (E < 0.1E^*) \end{aligned} \quad (2)$$

The transition energy  $E^*$  can be evaluated from the Larmor radius and the field coherence length  $r_L(E^*) = L_c/2\pi$ , giving:

$$E^* \simeq 1.45 \times 10^{20} \left( \frac{B}{\mu\text{G}} \right) \left( \frac{L}{\text{Mpc}} \right) \text{eV}$$

Of course, the transition actually takes place over a range of energies around  $E^*$ .

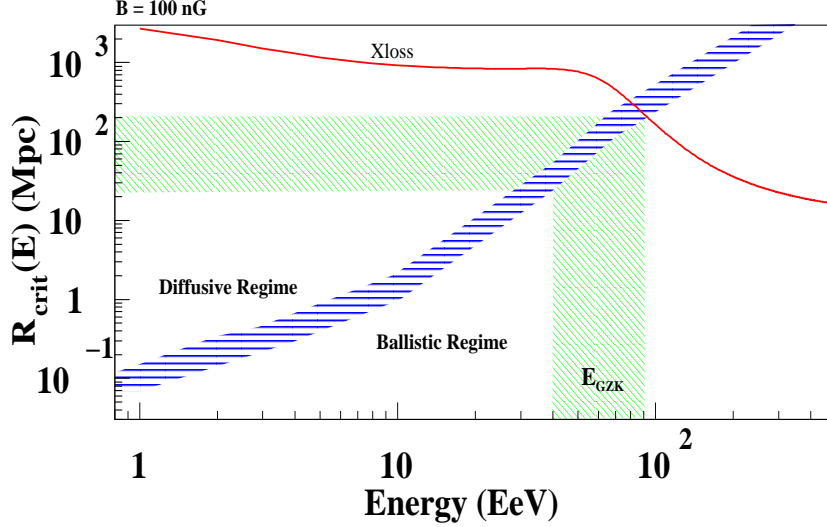


Fig. 2. Regions in the plane ( $E - R$ ) where ballistic or diffusive regime describes particle trajectories for a 100 nG field. The transition occurs around a few tens of Mpc, i.e. inside the GZK sphere at GZK energies.

Below the GZK cutoff energy, where losses do not play a crucial role, the Green function for the diffusion is given by:

$$n(E, \vec{r}, t) = \frac{N_0}{(8\pi D(E)t)^{3/2}} \exp\left(-\frac{r^2}{4D(E)t}\right)$$

From this solution, one can estimate the radius of the diffusion sphere as a function of time and energy:

$$R(E, t) \sim \sqrt{4D(E)t}$$

For a given source distance  $R$ , the energy scale separating the ballistic and diffusive regimes can be estimated by comparing the corresponding propagation times:  $R^2/4D(E_c)$  and  $R/c$ . Fig. 2 shows this energy as a function of source distance for a random field of 100 nG. It is remarkable that for sources within the GZK sphere (10–100 Mpc), the transition occurs around the GZK energy (i.e. a few tens of EeV).

The existence of a diffusion sphere whose radius grows much slower than  $ct$  gives rise to a *magnetic horizon* which limits the distance up to which a given particle can escape from its source before losing most of its energy. This horizon is given by:

$$R_H = \sqrt{4D(E)T_{loss}(E)} \quad (3)$$

where  $T_{loss}(E) = E/\frac{dE}{dt}$  is the energy loss time.

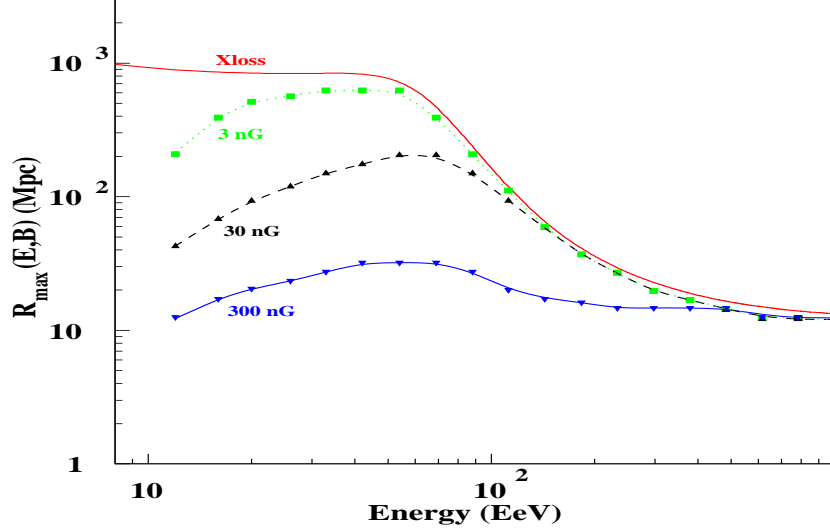


Fig. 3. Magnetic horizon as a function of energy for various field strengths. The horizon is defined as the radius of the sphere enclosing 68% of the particles trajectories. The maximum propagation time is fixed by the energy loss time (top solid line). One can see that for a 300 nG random field, the horizon is fairly constant around 20 Mpc at all energies.

Using the Monte Carlo described in the previous section, we computed this distance as the maximum radius reached by 68% of the particles over a propagation time  $T_{loss}(E)$ . This horizon is shown on Fig. 3. At lower energy (below 10 EeV), it is given by Eqn. 3 and the parameterization of the diffusion coefficients given in Eqn. 2. Different values of turbulent magnetic fields have been used. For relatively strong fields (300 nG), the horizon is the same before and after the GZK energy ; implying that the sudden reduction of the visible Universe at the origin of the expected suppression of the flux above 100 EeV does *not* occur in that case.

## 4 Results

All the following results have been obtained for continuous sources with power-law injection spectra of index 2.3 and maximum energy of 1000 EeV. This slope is typical of particle acceleration at relativistic shockwave [14,15,16].

We calculated the observed spectra for various source positions (45 values distributed uniformly in log scale from 1 Mpc to 1 Gpc) and turbulent field values ranging from 3 to 300 nG. Fig. 4 shows a comparison of these spectra for sources at 1, 10, 50 and 100 Mpc obtained with a 100 nG random field. The solid angle effect has been taken away so that the normalization and spectra at all distances would be identical in the absence of magnetic field and energy losses. As expected, the spectrum of a very close source (1 Mpc)

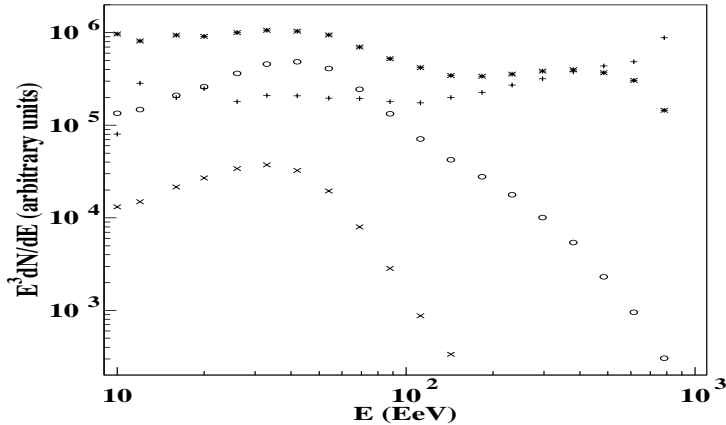


Fig. 4. Comparison of spectra obtained for sources located at 1 (+), 10 (\*), 50 (o) and 100 (x) Mpc in a turbulent field of 300nG. The solid angle effect has been taken away, so that the normalization of the four spectra would be identical in the absence of magnetic field and energy losses. As expected, the GZK cutoff is visible for far away sources, but the latter have a negligible contribution to the total flux at all energies.

shows a softening (index changing from  $-2.3$  to about  $-3.0$ ) at low energies due to the accumulation of low energy particles, while at high energy the original spectrum is restored. For such a nearby source there is of course no GZK cutoff, but this configuration would lead to an anisotropy in the sky incompatible with the already available data. At intermediate distance (10 Mpc) the flux is only slightly reduced at high energy and the contribution (corrected by  $E^3$ ) at 10 EeV and 1000 EeV are roughly the same, leading to a nearly flat spectrum in the 10–1000 EeV range.

Further away (above 100 Mpc) the flux is strongly attenuated at high energy because of the GZK cutoff but also at low energy because of the diffusive regime. One should also note that increasing the distance between the source and the observer leads to a stronger GZK cutoff because the mean travel length increases faster than the source distance. Moreover, for greater source distances, the diffusive regime extends to higher energy, as shown by Fig. 2.

The main conclusion is therefore that far away sources have a negligible contribution to the total flux at *all* energies (and not only above GZK energy). In other words, the presence of random magnetic fields leads to a non trivial configuration of sources contributing to the spectrum, even in the case of a uniform distribution.

In Fig. 5 we compare the observed flux for a uniform distribution of sources between 10 and 1000 Mpc with and without a 300 nG random magnetic field.



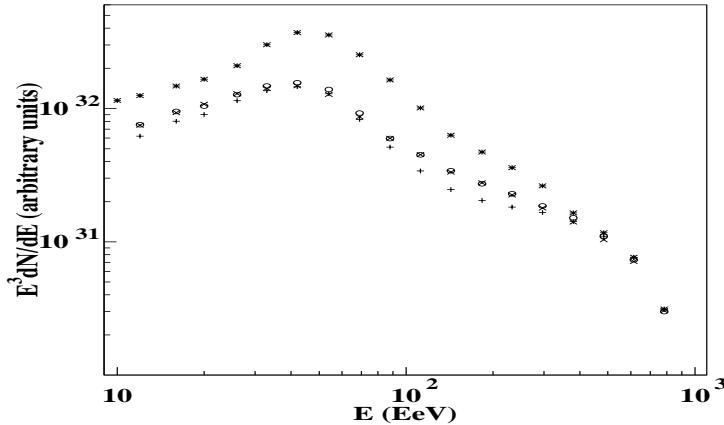


Fig. 5. Spectrum for a uniform distribution of sources between 10 and 1000 Mpc without random magnetic field ( $\star$ ) and in the presence of a 300 nG field (+). In the later case the low energy part of the spectrum is reduced leading to a flattening of the GZK cutoff. Also shown are the spectra ( $o$  and  $\times$ ) corresponding to non uniform fields, with alternated voids and sheets regions (see text).

In the later case the reduction of the low energy flux is clearly visible as the observer lies mostly outside the diffusion spheres. The exact form of the spectrum strongly depends on the source configuration on a scale (a few tens of Mpc) where the Universe cannot be taken as uniform. Therefore the local configuration of sources may lead to a spectrum that lies anywhere between the shapes of those obtained from individual sources at 10 or 50 Mpc as shown on Fig. 4.

This comparison also shows that for a field of 300 nG, propagation becomes purely ballistic only above 500 EeV and the transition between the diffusive and ballistic regimes spreads over half a decade above 100 EeV. This transition implies a flattening of the spectrum at energies higher than  $E_{GZK}$ . The position of this flattening strongly depends on the position of the most contributing sources, and on the value of random fields. Increasing the value of the random fields ( $\geq 3\mu\text{G}$ ) leads to particle diffusion on small scales (a few tens of Mpc) even at energies higher than  $E_{GZK}$ , and therefore moves the transition to the ballistic regime to energies so high ( $> 10^{21}$  eV) that this transition becomes invisible. In such a situation a strong GZK cutoff is restored as the signature of the much shorter energy loss time of post GZK particles.

## 5 Conclusion

We have modelled a fully magnetized Universe to study the effect of random magnetic fields on the spectra of UHECR sources, in a spherically symmetric Universe, in order to get rid of any additional effect related to the geometry of magnetic fields and source distributions. We showed that for magnetic fields in the 100 nG range, sources more distant than about 100 Mpc do not contribute to the observed fluxes at *all* energies. In such a model, the argument of the GZK cutoff in its original form in terms of a sudden reduction of the horizon is modified.

We are aware that a fully magnetized Universe is not a realistic model of our environment. Voids are known to exist, where random fields would rather be around a few nG, or more less. In such regions, UHECRs propagate ballistically even at low energies where GZK losses are unimportant, and therefore the particular effect which we discussed above does not appear. However, our main argument that *"far away sources do not contribute to the visible spectrum of UHECRs at all energies"* would be maintained if all sources are surrounded by a random field of order 100 nG over distances of several Mpc, as expected for sources that lie within galaxies or clusters.

By using a locally homogeneous Universe, we implicitly restricted ourselves to one sheet of magnetic fields and neglected the contribution of other high-density sheets that may lie in our neighbourhood. While this is a direct consequence of our choice to isolate the ‘magnetic cutoff’ effect from any other effect influencing the shape of the spectrum, it may also be qualitatively justified by the fact that the highest energy particles would not be able to travel the distances between two neighbouring sheets without losing some energy, and the lowest energy particles would be largely reflected as they approach the strongly enhanced magnetic fields in our own sheet, resulting in a reduced flux contribution. Such an (imperfect) confinement of UHECRs between two magnetic walls contributes to isolate regions of high magnetic fields from one another.

To illustrate the effect of non uniform fields, with alternating voids and sheets, we also investigated models in which the fields are concentrated in gaussian concentric shells of width  $\sigma = 5 \text{ Mpc}/\sqrt{2}$  (as in the description of planar magnetic sheets in Ref. [7]) or  $\sigma = 2 \text{ Mpc}/\sqrt{2}$ , and radii increasing by steps of 30 Mpc, respectively 15 Mpc. As shown in Figure 5, the reduction of the low energy part of the spectrum (between  $10^{19}$  and  $10^{20}$  eV) is still visible in this field configuration, and the general effect of reducing the GZK suppression remains. More realistic field configurations thus do not seem to affect the general arguments emphasized here.

We did not model any particular configuration of sources to study the anisotropy effect, but given the slowness of the transition between the two propagation regimes and the fact that the transport becomes only purely ballistic above 500 EeV, we expect that anisotropies would be visible only above 100 EeV where the data is currently too scarce for one to make any definitive statement. It has been shown recently that even with more localized magnetic fields the expected anisotropy from local sources is not ruled out by the current data [18]. One should also note that a few sources localized in the magnetic sheet around the local supercluster would suppress the bump before  $E_{GZK}$ , visible on Fig. 5, because low-energy particles leak through the walls [7].

## Acknowledgments

We would like to thank Ricardo Perez for invaluable discussions.

## References

- [1] K. Greisen, Phys. Rev. Lett. 16 (1966) 748; G. T. Zatsepin and V. A. Kuzmin, Pis'ma Zh. Eksp. Teor. Fiz. 4 (1966) 114 [JETP. Lett. 4 (1966) 78].
- [2] P. P. Kronberg, Reports of Progress in Physics 58 (1994) 325; J. P. Vallée, Fundamentals of Cosmic Physics, Vol. 19 (1997) 1; T. E. Clarke, P. P. Kronberg, and H. Böhringer, Astrophys. J. Lett. 547 (2001) L111; J.-L. Han and R. Wielebinski, e-print astro-ph/0209090.
- [3] D. Ryu, H. Kang, and P. L. Biermann, Astron. Astrophys. 335 (1998) 19.
- [4] P. Blasi, S. Burles, and A. V. Olinto, Astrophys. J. 514 (1999) L79.
- [5] for a recent review see P. P. Kronberg, Physics Today 55, December 2002, p. 40.
- [6] J. Wdowczyk, A.W. Woldendale, Nature 281 (1979) 356.
- [7] G. Sigl, M. Lemoine, and P. Biermann, Astropart. Phys. 10 (1999) 141.
- [8] C. Isola, M. Lemoine, and G. Sigl, Phys. Rev. D 65 (2002) 023004.
- [9] T. Stanev, D. Seckel, and R. Engel, e-print astro-ph/0108338; see also T. Stanev, R. Engel, A. Mucke, R. J. Protheroe, and J. P. Rachen, Phys. Rev. D 62 (2000) 093005.
- [10] P. Blasi and A.V. Olinto, Phys. Rev. D 59 (1999) 023001.
- [11] G. Medina-Tanco, Lect. Notes Phys. 576 (2001) 155.
- [12] F.Casse, *Thèse de doctorat*, Université de Grenoble, 2001.

- [13] F.Casse, M.Lemoine, G.Pelletier, Phys.Rev. D65 (2002) 023002, arXiv:astro-ph/0109223
- [14] D.C. Ellison, G.P. Double, Astroparticle Physics 18 (2002) 213
- [15] A. Achterberg, Y.A. Gallant, J.G. Kirk, A.W. Guthmann, MNRAS 2001, 328, 393
- [16] M. Lemoine, G. Pelletier, 2003, ApJ, 589, L73
- [17] C. Isola and G. Sigl, Phys. Rev. D 66 (2002) 083002.
- [18] G.Sigl, F. Miniati, T.A.Enßlin, astro-ph/0302388